Fixed-Phase Diffusion Monte Carlo Study of the Quantum Hall Effect on the Haldane Sphere

V. Melik-Alaverdian and N. E. Bonesteel

National High Magnetic Field Laboratory and Department of Physics, Florida State University, Tallahassee, FL 32306-4005

G. Ortiz

Theoretical Division, Los Alamos National Laboratory, P.O. Box 1663, Los Alamos, NM 87545

(August 22, 1997)

Abstract

A generalized diffusion Monte Carlo method for solving the many-body Schrödinger equation on curved manifolds is introduced and used to perform a 'fixed-phase' simulation of the integer and fractional quantum Hall effect on the Haldane sphere. The effect of Landau level mixing on the $\nu = 1$ and $\nu = 1/3$ energy gaps and the relative stability of spin-polarized and spin-reversed quasielectron excitations are studied using the new method.

Typeset using REVTEX

I. INTRODUCTION

Recently, Ortiz, Ceperley, and Martin (OCM) [1] introduced the 'fixed-phase' approximation for simulating non-time-reversal symmetric systems with complex valued eigenfunctions. Within this approximation the overall phase of a given trial wave function is 'fixed', and the optimal amplitude of the wave function obtained by numerically solving an effective time-reversal symmetric bosonic problem. OCM applied this method to the quantum Hall effect (QHE) using the torus geometry and fixing the phase of the wave function with Laughlin's trial wave function. The results were then used to study the effect of Landau level mixing (LLM) on the Wigner crystallization of fractional QHE fluids. However, OCM did not consider either excited states or geometries other than the torus.

In this paper we present the results of a fixed-phase diffusion Monte Carlo (DMC) study of the QHE at Landau level filling fractions $\nu = 1$ and $\nu = 1/3$ using the spherical geometry introduced by Haldane [2]. In order to use the Haldane sphere, arguably the most convenient geometry for numerical study of the QHE, we have developed a generalized DMC method for solving the many-body Schrödinger equation on curved manifolds. Using this new method we have calculated the effect of LLM on the QHE transport gap, *i.e.*, the energy gap for creating a quasielectron – quasihole pair with infinite separation, obtaining results for both spin-polarized and spin-reversed [3,4] quasielectrons.

II. THE TWO DIMENSIONAL ELECTRON GAS ON THE HALDANE SPHERE

An ideal two dimensional electron gas, with effective mass m^*, carrier density n and dielectric constant ϵ, placed in a transverse magnetic field B is characterized by three length scales — the effective Bohr radius $a_B = \epsilon\hbar^2/m^*e^2$, the magnetic length $l_0 = \sqrt{\hbar c/eB}$, and the mean interparticle spacing $d = 1/\sqrt{\pi n}$. These length scales can be combined to form two independent dimensionless ratios, the filling factor $\nu = 2l_0^2/d^2$, and the electron gas parameter $r_s = d/a_B$. The degree of LLM is characterized by the ratio of the typical

Coulomb energy to the cyclotron energy $(e^2/\epsilon d)/\hbar\omega_c = r_s\nu/2$ where $\omega_c = eB/m^*c$. Thus, for fixed ν, r_s provides a useful measure of the importance of LLM. Because $r_s \propto m^*/\sqrt{B}$ LLM can be increased either by decreasing B or increasing m^*. For example, in two dimensional GaAs/AlGaAs systems with typical carrier densities, for n-type systems $m^* \simeq 0.07$ and $r_s \sim 2$ while for p-type systems $m^* \simeq 0.38$ and $r_s \sim 10$.

In the spherical geometry electrons are confined to the surface of a sphere of radius R with a magnetic monopole at its center. Let N denote the number of electrons and $2S$ denote the number of flux quanta piercing the surface of the sphere. The field strength is then $B = S\hbar c/eR^2$ and, for $\nu = 1/q$, $2S = q(N-1)$. If electron positions are given in stereographic coordinates, $\mathbf{r} = (x, y) = (\cos\phi, \sin\phi)\tan\theta/2$ where θ and ϕ are the usual spherical angles, then the Hamiltonian is, in appropriately scaled atomic units ($\hbar = m^* = e = 1$),

$$H = \frac{1}{2}\sum_i D(\mathbf{r}_i)(-i\nabla_i + \mathbf{A}(\mathbf{r}_i))^2 + \frac{1}{\epsilon}\sum_{i<j}\frac{1}{\sqrt{r_{ij}^2 + \beta^2}} \ , \tag{1}$$

where $D(\mathbf{r}_i) = (1 + r_i^2)^2/4R^2$, r_{ij} is the chord distance on the sphere, and β is a parameter which models the finite thickness of the 2DEG [5]. We work in the Wu-Yang [6] gauge for which $\mathbf{A}(\mathbf{r}_i) = 2R^2B(-y_i, x_i)/(1 + r_i^2)$.

III. FIXED-PHASE APPROXIMATION

The fixed-phase approximation is carried out as follows. First, a given trial function is written as $\psi_\mathrm{T}(\mathcal{R}) = |\psi_\mathrm{T}(\mathcal{R})| \ \exp[i\phi_\mathrm{T}(\mathcal{R})]$, where $\mathcal{R} = (\mathbf{r}_1, \mathbf{r}_2, \cdots, \mathbf{r}_N)$. The overall phase $\phi_\mathrm{T}(\mathcal{R})$ is then used to perform a singular gauge transformation, $\hat{H} = \exp[-i\phi_\mathrm{T}(\mathcal{R})] \ H \ \exp[i\phi_\mathrm{T}(\mathcal{R})] = H_\mathrm{R} + iH_\mathrm{I}$, where

$$H_\mathrm{R} = -\frac{1}{2}\sum_i D(\mathbf{r}_i)(\nabla_i^2 - \tilde{\mathbf{A}}^2(\mathbf{r}_i)) + \frac{1}{\epsilon}\sum_{i<j}\frac{1}{\sqrt{r_{ij} + \beta^2}}, \tag{2}$$

$$H_\mathrm{I} = -\frac{1}{2}\sum_i D(\mathbf{r}_i)\left(\nabla_i \cdot \tilde{\mathbf{A}}(\mathbf{r}_i) + \tilde{\mathbf{A}}(\mathbf{r}_i) \cdot \nabla_i\right) \ , \tag{3}$$

and $\tilde{\mathbf{A}}(\mathbf{r}_i) = \mathbf{A}(\mathbf{r}_i) + \nabla_i \phi_{\rm T}(\mathcal{R})$. As shown by OCM, the bosonic ground state of $H_{\rm R}$ is the lowest energy state with the same phase as the trial function [1].

For the present calculations we have used three trial wave functions to implement the fixed-phase approximation ($z = x + iy$ is the complex stereographic coordinate):

(i) Ground state.— In the Wu-Yang gauge the spherical analog of the Laughlin wave function for $\nu = 1/q$ is [2]

$$\psi_{\rm GS} = \prod_k (1 + |z_k|^2)^{-S} \prod_{i<j} (z_i - z_j)^q \; . \tag{4}$$

(ii) Spin-polarized excited state.— For this state we have used the following wave function, constructed using Jain's composite fermion approach [7], describing an excitation with a charge e/q quasielectron at the top of the sphere and a charge $-e/q$ quasihole at the bottom of the sphere,

$$\psi_{\rm SP} = \prod_k (1 + |z_k|^2)^{-S} \prod_{i<j} (z_i - z_j)^{q-1} \begin{vmatrix} 1 & z_1 & \ldots & z_1^{N-2} & \sum_{i \neq 1} \frac{1}{z_1 - z_i} \\ \vdots & \vdots & & \vdots & \vdots \\ 1 & z_N & \ldots & z_N^{N-2} & \sum_{i \neq N} \frac{1}{z_N - z_i} \end{vmatrix} \; . \tag{5}$$

(iii) Spin-reversed excited state.— This state is similar to $\psi_{\rm SP}$ except the quasielectron has a reversed spin. If z_1 denotes the coordinate of the down spin electron then this wave function is [4]

$$\psi_{\rm SR} = \prod_k (1 + |z_k|^2)^{-S} \prod_{l \neq 1} (z_l - z_1)^{-1} \prod_{i<j} (z_i - z_j)^q \; . \tag{6}$$

IV. DIFFUSION MONTE CARLO ON THE SPHERE

By applying the fixed-phase approximation a many-fermion system in a magnetic field is transformed into an effective, time-reversal symmetric, bosonic system. For this transformed system there is no 'sign problem' and standard numerical techniques can be applied. Here, as in OCM, we apply the DMC method. This method, reviewed in [8], is based on the observation that $\psi(\mathcal{R}, t)$, the solution of the imaginary-time Schrödinger equation

$H_{\rm R}\psi(\mathcal{R},t) = -\frac{\partial}{\partial t}\psi(\mathcal{R},t)$, converges to the ground state of $H_{\rm R}$ in the limit $t \to \infty$. In imaginary time the Schrödinger equation for the present problem becomes a diffusion equation with a position dependent diffusion 'constant' $D(\mathbf{r})$. This dependence on position is a consequence of the finite curvature of the surface of the sphere, for which the metric tensor, in stereographic coordinates, is $g_{\alpha\beta}(\mathbf{r}) = D(\mathbf{r})^{-1}\delta_{\alpha\beta}$. Note that in two dimensions it is always possible to choose coordinates for which $g_{\alpha\beta} = f(\mathbf{r})\delta_{\alpha\beta}$, *i.e.*, to work in the so-called 'conformal gauge', and so the generalized DMC method introduced below can, in principle, be applied to *any* curved two-dimensional manifold, not just the sphere.

The central modification of the DMC method required here is to replace the usual importance-sampled distribution function $P(\mathcal{R},t) = \psi(\mathcal{R},t)|\psi_{\rm T}(\mathcal{R})|$ [8] with

$$\widetilde{P}(\mathcal{R},t) = \psi(\mathcal{R},t)|\psi_T(\mathcal{R})| \prod_{i=1}^{N} \frac{1}{D(\mathbf{r}_i)} \; . \tag{7}$$

This has two important consequences. First, because the differential area element on the sphere is $dA = d^2r/D(\mathbf{r})$ the expectation value of the ground state energy is simply

$$\langle H \rangle = \frac{\int \widetilde{P}(\mathcal{R}, t \to \infty) E_L(\mathcal{R}) d\mathcal{R}}{\int \widetilde{P}(\mathcal{R}, t \to \infty) d\mathcal{R}} \; . \tag{8}$$

Second, the differential equation satisfied by $\widetilde{P}(\mathcal{R},t)$ is,

$$-\frac{\partial}{\partial t}\widetilde{P}(\mathcal{R},t) = \sum_{i=1}^{N}\left[-\frac{1}{2}\nabla_i^2(D(\mathbf{r}_i)\widetilde{P}(\mathcal{R},t)) + \nabla_i\cdot(D(\mathbf{r}_i)\mathbf{F}_i(\mathcal{R})\widetilde{P}(\mathcal{R},t))\right] + (E_L(\mathcal{R}) - E_T)\widetilde{P}(\mathcal{R},t) \; , \tag{9}$$

where $\mathbf{F}_i(\mathcal{R}) = \nabla_i \ln|\psi_T|$, $E_L(\mathcal{R}) = H_{\rm R}|\psi_{\rm T}|/|\psi_{\rm T}|$ and E_T is a constant which must be adjusted in the course of the simulation to be equal to the ground state energy. It is worth noting that, except for the position dependence of $D(\mathbf{r})$, (9) has the same form as the usual diffusion equation appearing in DMC simulations [8].

Equation (9) can be solved numerically by stochastically iterating the integral equation

$$\widetilde{P}(\mathcal{R}', t+\tau) = \int G(\mathcal{R} \to \mathcal{R}', \tau)\widetilde{P}(\mathcal{R},t) d\mathcal{R} \; , \tag{10}$$

using the short-time propagator ($\mathcal{O}(\tau^2)$)

$$G(\mathcal{R} \to \mathcal{R}', \tau) = \exp\left[-\tau\left(\frac{[E_L(\mathcal{R}) + E_L(\mathcal{R}')]}{2} - E_T\right)\right] \prod_{i=1}^{N} G_i^0(\mathcal{R} \to \mathcal{R}', \tau) \; , \tag{11}$$

where

$$G_i^0(\mathcal{R} \to \mathcal{R}', \tau) = \frac{1}{2\pi D(\mathbf{r}_i)\tau} \exp\left[\frac{-(\mathbf{r}_i' - \mathbf{r}_i - D(\mathbf{r}_i)\tau\mathbf{F}_i(\mathcal{R}))^2}{2D(\mathbf{r}_i)\tau}\right] \tag{12}$$

represents a diffusion and drift process. In (12) both $D(\mathbf{r}_i)$ and $F_i(\mathcal{R})$ are evaluated at the 'prepoint' in the integral equation. This makes it possible to simulate (10) in terms of branching random walks by a straightforward application of the DMC algorithm given in [8], and is a direct consequence of having the spatial derivatives in (9) sit all the way to the left in each term [9]. This in turn follows from our modified definition of $\widetilde{P}(\mathcal{R}, t)$. Had we used the usual definition, $P(\mathcal{R}, t)$, we would have obtained 'quantum corrections' in the propagator [9,10].

V. RESULTS

The r_s dependence of the ground state energy, and the energies of the spin-polarized and spin-reversed excited states, have been calculated by applying the fixed-phase approximation using the trial functions $\psi_{\rm GS}$, $\psi_{\rm SP}$ and $\psi_{\rm SR}$, respectively, and solving the resulting bosonic problems using the generalized DMC method outlined above. An important test of our method is shown in Fig. 1. In this figure the $\nu = 1/3$ ground state energy as a function of r_s for $\beta = 0$ is compared to the variational Monte Carlo results of Price *et al.* [11]. The wave functions used in the variational calculations have the same phase as $\psi_{\rm GS}$ and so must have higher energies than our fixed-phase DMC results, as can be seen to be the case.

A. Energy Gap: $\nu = 1$

Mixed estimates [8] of the the density profile of the spin-reversed excited state at $\nu = 1$ are shown in Fig. 2 for $N = 20$ and $r_s = 0$, 1 and 20. The excess charge at the top of the sphere ($\theta = 0$) is the spin-reversed quasielectron, and the charge deficit at the bottom of the sphere ($\theta = \pi$) is the (spin-polarized) quasihole. When $r_s = 0$ there is an exact $\nu \leftrightarrow 2 - \nu$ particle-hole symmetry which relates the $\nu = 1$ spin-reversed quasielectron to the spin-polarized quasihole. This symmetry can clearly be seen in the density profile for $r_s = 0$, as can the breaking of this symmetry due to LLM with increasing r_s.

The $\nu = 1$ spin-reversed energy gap, $\Delta_{\rm SR}$, obtained by subtracting the ground state energy from the spin-reversed excited state energy without the Zeeman contribution, is plotted vs. r_s in Fig. 3. The results are for $N = 20$ and zero thickness ($\beta = 0$). For $r_s = 0$ there is no LLM and $\Delta_{\rm SR} = \sqrt{\frac{\pi}{2}}\frac{e^2}{\epsilon l_0} \simeq 1.25\frac{e^2}{\epsilon l_0}$ [12]. As r_s increases $\Delta_{\rm SR}$ decreases rapidly, in agreement with the variational calculations of Králik *et al.* [13]. It is generally believed that the relevant excited state at $\nu = 1$ is not this simple spin-reversed excitation, but a more extended Skyrmion spin texture [14]. The strong r_s dependence of the spin-reversed energy gap found here suggests that LLM may have a significant effect on the stability and size of the Skyrmion, and work is currently underway to investigate this.

B. Energy Gap: $\nu = 1/3$

The $\nu = 1/3$ spin-polarized and spin-reversed energy gaps, $\Delta_{\rm SP}$ and $\Delta_{\rm SR}$, obtained by subtracting the ground state energy from the relevant excited state energies, are plotted vs. r_s in Fig. 4. Results are for $N = 20$ and are given for $\beta = 0$ and the more experimentally relevant case $\beta = 1.5\ l_0$. The additional Zeeman energy of the spin-reversed excitation is not included in our definition of $\Delta_{\rm SR}$, and so the crossover magnetic field, B_c, below which the spin-reversed excitation has lower energy than the spin-polarized excitation, is $B_c = (\Delta_{\rm SP} - \Delta_{\rm SR})/g\mu_B$, where μ_B is the Bohr magneton and g is the effective g-factor. For GaAs ($\epsilon \simeq 13, g \simeq 0.5$) we find, for $r_s = 2$, $B_c \simeq 14$ T, while for $r_s = 10$, $B_c \simeq 7$ T. This reduction of B_c with increasing r_s reflects the fact that, for $\beta = 0$, LLM has a significantly stronger effect on $\Delta_{\rm SP}$ than on the $\Delta_{\rm SR}$, and so tends to stabilize the spin-polarized excitation.

For the more experimentally relevant case $\beta = 1.5\ l_0$ the effect of LLM on $\Delta_{\rm SP}$ and $\Delta_{\rm SR}$ is much weaker than for $\beta = 0$ and the difference in the two gap energies, in units of $e^2/\epsilon l_0$, is roughly constant. Again using GaAs parameters we find $B_c \simeq 4$ T for $r_s = 2$ and $B_c \simeq 3$

T for $r_s = 10$. This result for the crossover field is in reasonable agreement with previous calculations which included the thickness correction but not LLM [3,4]. The new result here is that, when thickness is included, B_c is only weakly dependent on LLM.

Figure 5 shows mixed estimates [8] of the density profiles of the spin-polarized and spin-reversed excited states at $\nu = 1/3$ as a function of θ for $r_s = 1$ and $r_s = 20$. The results are for $N = 20$ and $\beta = 0$. Note that for $r_s = 20$ the quasielectron and quasihole induce ripples in the density. This is a consequence of the increased Wigner crystal-like correlations in the FQHE fluid induced by LLM.

The effect of LLM on Δ_{SP} and Δ_{SR} can be understood qualitatively using Fig. 5 as follows. For the spin-polarized state the quasielectron charge is concentrated in a ring centered at the top of the sphere. As r_s increases this ring of charge spreads out and the dip at $\theta = 0$ deepens. This evolution of the quasielectron charge occurs because, as higher Landau levels are mixed into the wave function, the charge is free to spread out, lowering its Coulomb energy at the cost of some kinetic energy. For the spin-reversed quasielectron the charge is spread out more uniformly and the Coulomb energy is less than that of the spin-polarized quasielectron. There is therefore less of a tendency for the spin-reversed quasielectron charge to spread out with increasing r_s, and so this excitation is less affected by LLM. The weakening of the effect of LLM on the energy gaps due to the thickness correction can also be understood along similar lines. For $\beta = 1.5\ l_0$ the short-range part of the Coulomb interaction is softened, and the potential energy of both the spin-reversed and spin-polarized quasielectrons are reduced. There is therefore less of a tendency for the charge of these excitations to spread out with increasing r_s, and so, again, the effect of LLM is weakened.

For typical carrier densities the magnetic field at $\nu = 1/3$ is greater than B_c and the transport gap is set by Δ_{SP}. This gap has been measured in both n-type [15] and p-type [16] GaAs quantum wells, with typical results, for the highest quality samples, of $\Delta_{\mathrm{n}} \simeq 0.05e^2/\epsilon l_0$ and $\Delta_{\mathrm{p}} \simeq 0.023e^2/\epsilon l_0$, respectively. The factor of 2 reduction of the energy gap from n-type ($r_s \sim 2$) to p-type ($r_s \sim 10$) samples has been attributed to the increased LLM [16].

However, our results show that LLM has only a weak effect on $\Delta_{\rm SP}$ when the thickness effect is included, in agreement with previous calculations [11,17,18]. Thus, while our energy gap for $r_s \simeq 2$ is close to the experimental value, our result for $r_s \simeq 10$ is off by roughly a factor of 2. This discrepancy between theory and experiment is most likely due to disorder, the effects of which on the energy gap are still poorly understood.

VI. CONCLUSIONS

To conclude, a generalized DMC method for solving the many-body Schrödinger equation on curved manifolds has been introduced and used to perform a 'fixed-phase' simulation of the FQHE on the Haldane sphere. The effect of LLM on the $\nu = 1$ and $\nu = 1/3$ energy gaps, and the relative stability of the spin-polarized and spin-reversed quasielectron states have been investigated using the new method.

The authors would like to thank D. Ceperley and L. Engel for useful discussions. This work was supported by the U.S. Department of Energy under Grant No. DE-FG02-97ER45639 and by the National High Magnetic Field Laboratory at Florida State University. NEB acknowledges support from the Alfred P. Sloan foundation, and GO from an Oppenheimer fellowship.

REFERENCES

[1] G. Ortiz, D.M. Ceperley, and R.M. Martin, Phys. Rev. Lett. **71**, 2777 (1993).

[2] F.D.M. Haldane, Phys. Rev. Lett. **51**, 605 (1983).

[3] T. Chakraborty, P. Pietiläinen, and F.C. Zhang, Phys. Rev. Lett. **57**, 130 (1986).

[4] R. Morf and B.I. Halperin, Z. Phys. B **68** 391 (1987).

[5] F.C. Zhang and S. Das Sarma, Phys. Rev. B **33**, 2903 (1986).

[6] T.T. Wu and C.N. Yang, Nucl. Phys. B **107**, 365 (1976).

[7] J.K. Jain, Phys. Rev. Lett. **63**, 199 (1989); Phys. Rev. B **40**, 8079 (1989); *ibid.* **41**, 7653 (1990).

[8] P. J. Reynolds, D. M. Ceperley, B.J. Alder, and W. A. Lester, Jr., J. Chem. Phys. **77**, 5593 (1982).

[9] V. Melik-Alaverdian, G. Ortiz, and N.E. Bonesteel, in preparation.

[10] For a discussion of quantum corrections see, for example, B.S. DeWitt, Rev. Mod. Phys. **29**, 377 (1957); and D.W. McLaughlin and L.S. Schulman, J. Math. Phys. **12** 2520 (1971).

[11] R. Price, P.M. Platzman, and S. He, Phys. Rev. Lett. **70**, 339 (1993); R. Price and S. Das Sarma, Phys. Rev. B **54**, 8033 (1996).

[12] C. Kallin and B.I. Halperin, Phys. Rev. B **30**, 5655 (1984).

[13] B. Králik, A.M. Rappe, and S.G. Louie, Phys. Rev. B **52**, R11626 (1995).

[14] S.L. Sondhi, A. Karlhede, S.A. Kivelson, and E.H. Rezayi, Phys. Rev. B **47**, 16419 (1993).

[15] R.L. Willet, H.L. Stormer, D.C. Tsui, A.C. Gossard, and J.H. English, Phys. Rev. B **37**, 8476 (1988); For more recent measurements see R.R. Du *et al.*, Phys. Rev. Lett.

70, 2944 (1993), and references therein.

[16] H.C. Manoharan, M. Shayegan, and S.J. Klepper, Phys. Rev. Lett. **73**, 3270 (1994).

[17] D. Yoshioka, J. Phys. Soc. Jpn. **55**, 885 (1986).

[18] V. Melik-Alaverdian and N.E. Bonesteel, Phys. Rev. B **52**, R17032 (1995).

FIGURES

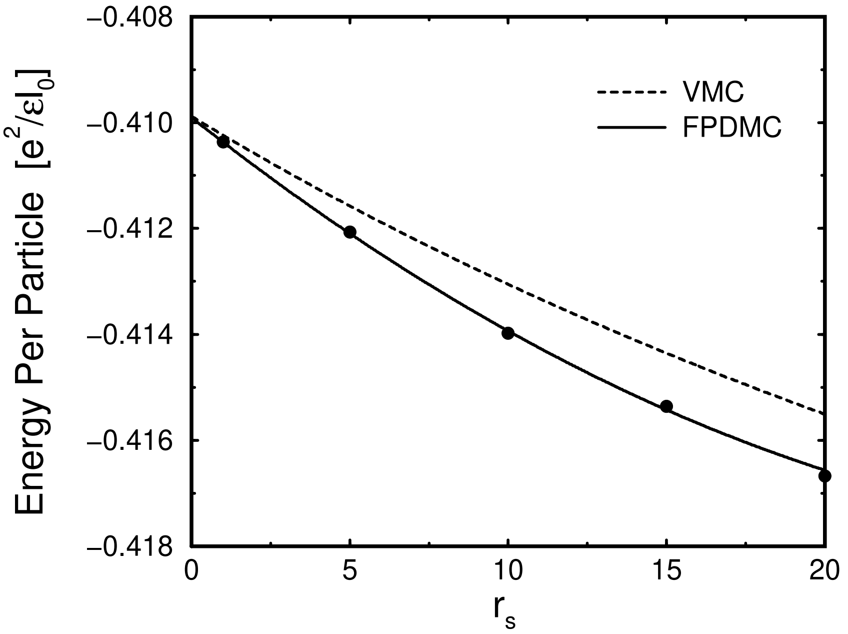

FIG. 1. Ground state energy per particle for $\nu = 1/3$ as a function of r_s. The dashed line is the variational result of Price *et al.* [11] and the solid line is a least square fit of a second degree polynomial in r_s to our fixed-phase DMC results for r_s = 1, 5, 10, 15 and 20 (dots). Statistical errors are smaller than symbol sizes.

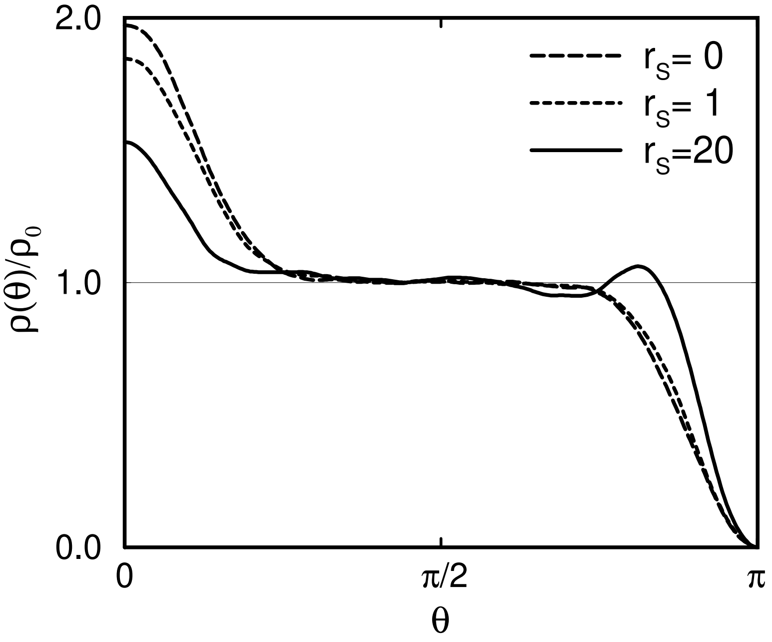

FIG. 2. Mixed estimate of the density profile of the $\nu = 1$ spin-reversed excited state on the sphere with a quasielectron at the top of the sphere ($\theta = 0$) and a quasihole on the bottom of the sphere ($\theta = \pi$) for $r_s = 0$, 1, and 20.

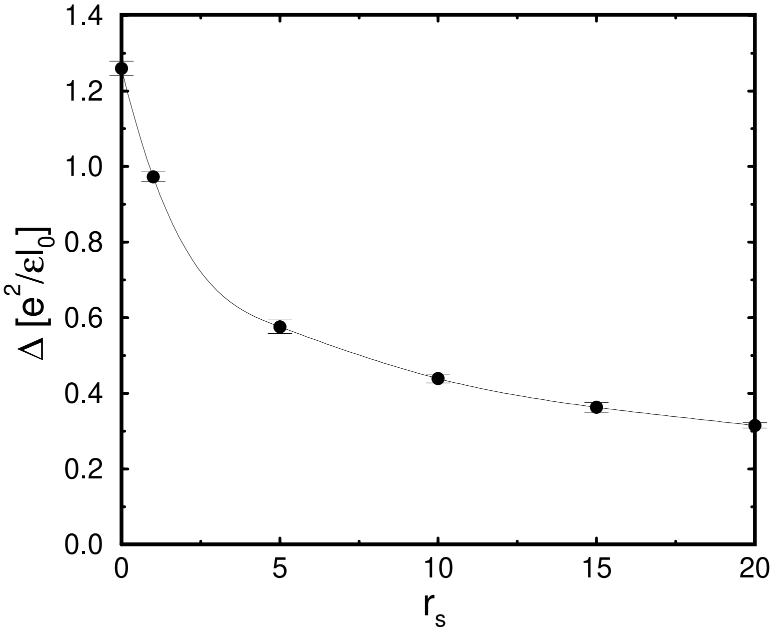

FIG. 3. $\nu = 1$ energy gap for creating a (spin-reversed) quasielectron-quasihole pair at opposite poles of the sphere vs. r_s. Results are for 20 electrons and $\beta = 0$ (zero thickness).

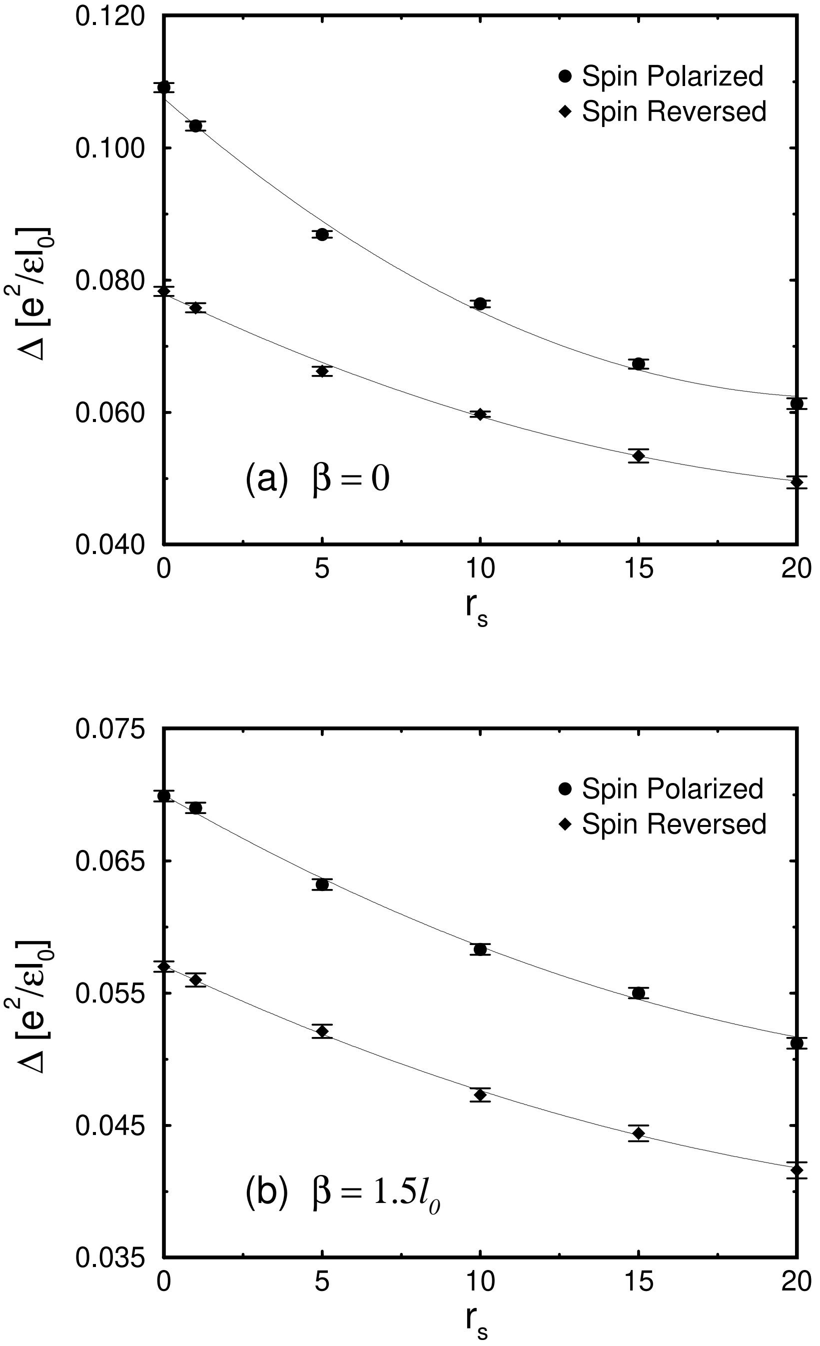

FIG. 4. $\nu = 1/3$ energy gaps for creating a quasielectron—quasihole pair at opposite poles of the sphere vs. r_s. Results are given for both a spin-polarized (dots) and spin-reversed (diamonds) quasielectron for thickness parameter *(a)* $\beta = 0$, and *(b)* $\beta = 1.5\ l_0$. Results are for 20 electrons.

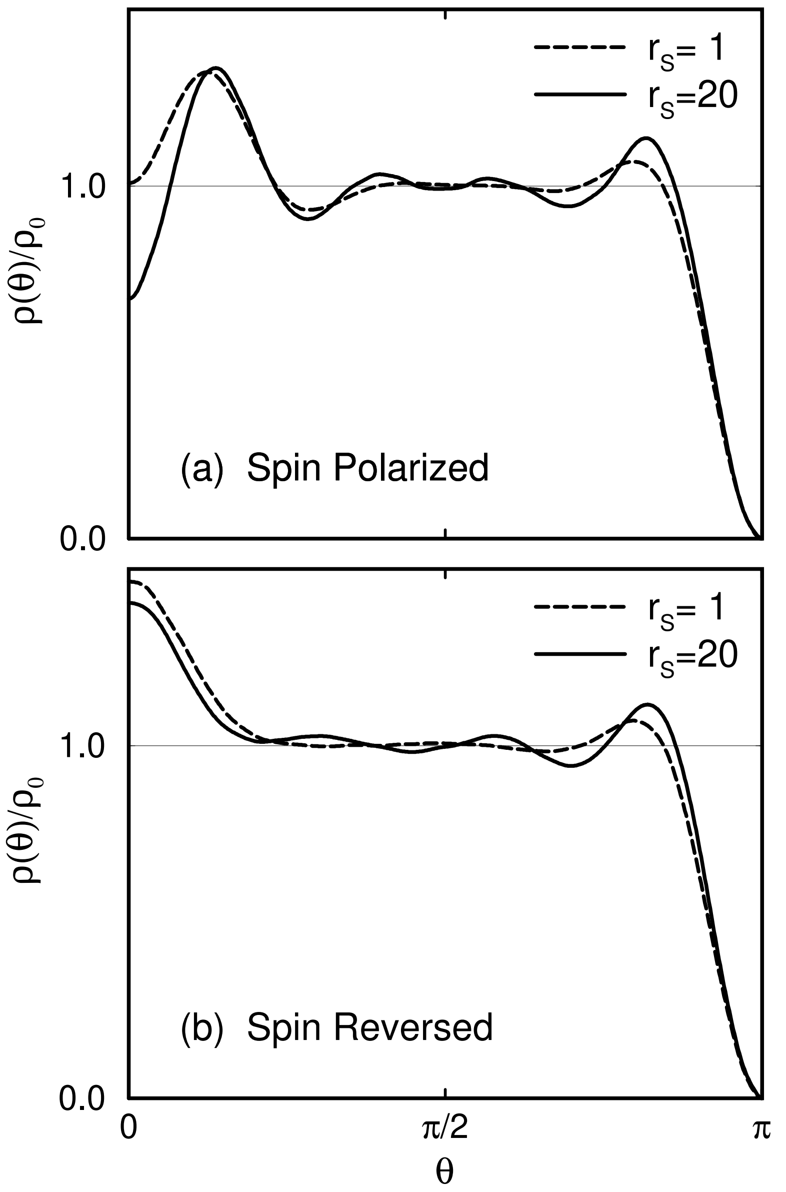

FIG. 5. Mixed estimates of the density profiles of $\nu = 1/3$ excited state wave functions on the sphere with a quasielectron at the top of the sphere ($\theta = 0$) and a quasihole on the bottom of the sphere ($\theta = \pi$) with $r_s = 1$ (dashed line) and $r_s = 20$ (solid line), for *(a)* the spin-polarized excited state, and *(b)* the spin-reversed excited state. Results are for 20 electrons.